A geometric switching approach toward thermal activation of metalloenediynes†

Sibaprasad Bhattacharyya, David F. Dye, Maren Pink and Jeffrey M. Zaleski*

Received (in Berkeley, CA, USA) 27th June 2005, Accepted 17th August 2005
First published as an Advance Article on the web 22nd September 2005
DOI: 10.1039/b509125j

Tetradentate metalloenediynes with strong imine and weaker thioether coordination serve as a geometrically non-rigid switch to drive thermal Bergman cyclization.

Transition metal catalyzed organic transformations usually rely on labilization of stable substrates prior to formation of the desired product. In much the same manner, transition metals have been shown to mediate enediyne reactivity, typically by enforcing a stabilizing or destabilizing effect on the ground or transition states by geometric or electronic structural modulation of the enediyne unit.[1–3] Indeed, metal oxidation state controlled tetrahedral and square planar metalloenediyne frameworks can have widely disparate thermal reactivities across each independent geometric construct.[4–10] However, beyond this, no straightforward means has been demonstrated to allow metal-mediated enediyne reactivity to be initiated by a change in conformation within a given metal oxidation state. To this end, herein we report the chemistry of a new tetradentate bis(quinolin-thio) enediyne that provides geometrically non-rigid N_2S_2 coordination at tetrahedral (Ag^+, Cu^+) and square planar/tetragonal centers (Cu^{2+}, Pd^{2+}). In the latter, heating permits transformation from a *trans*- to a *cis*-enediyne coordination geometry and formation of cyclized product at temperatures of ~100 °C below where they might be expected based on *trans* metalloenediyne structures.[11]

The tetradentate enediyne ligand (*Z*)-8-(8-(quinolin-8-ylthio)octa-4-en-2,6-diynylthio)quinoline (**1**) was prepared by reacting 1,8-dibromooct-4-ene-2,6-diyne with 2 equivalents of thioxine hydrochloride in DMF at RT (Scheme 1). The corresponding metal complexes of M^+ (M = Cu, Ag) and M^{2+} (M = Cu, Pd) were obtained by reaction of a 1 : 1 mixture of **1** and the appropriate metal salt in a 1 : 1 acetonitrile–chloroform solution (Scheme 2). In order to avoid possible polymer formation, all complexes were made in dilute solution by slow and simultaneous addition of ligand and metal salt solution.

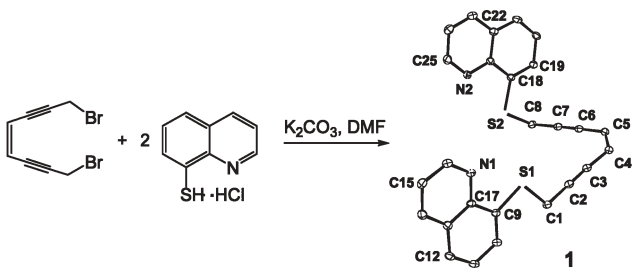

Scheme 1 Synthesis of tetradentate acyclic enediyne ligand **1**.

Department of Chemistry, Indiana University, Bloomington, IN, USA. E-mail: zaleski@indiana.edu; Fax: +1 (812) 855-8300; Tel: +1 (812) 855-2134

† Electronic supplementary information (ESI) available: Syntheses and characterizations of all compounds, as well as X-ray crystallographic data for **1**, **2**, **5**, **7**, and **8**. See http://dx.doi.org/10.1039/b509125j

The X-ray structure of acyclic ligand **1**‡ (Scheme 1) shows two spatially well separated quinoline moieties and a large alkyne termini separation (C2···C7, 4.32 Å). The alkyne angles show only slight distortion from linearity averaging ~175°.

The spherically symmetric d^{10} electronic configuration of Cu(I) complex **2** leads to a weakly distorted tetrahedral disposition of the ligand about the *cis*-CuN_2S_2 core (Fig. 1) as evidenced by a S1–Cu–S2 angle of 119°.§ Coordination decreases the alkyne termini separation (C2···C7) from 4.32 to 4.12 Å. The corresponding Ag(I) analogue **3** is expected to have a comparable coordination geometry and C2···C7 distance.[8]

In contrast, the d^8 electronic configuration of Pd(II) leads to a construct (**5**, Fig. 1) with square planar geometry.¶ Moreover, the unusual *trans* conformation of the enediyne ligand about Pd^{2+} leads to a C2···C7 distance that is *larger* than the tetrahedral structure of **3**, a situation that contradicts the established relationship between square planar (*cis*) and tetrahedrally coordinated enediynes. Similarly, based on thermal reactivity comparisons (*vide infra*) and the structures of other Cu(II) metalloenediynes, the Cu(II)

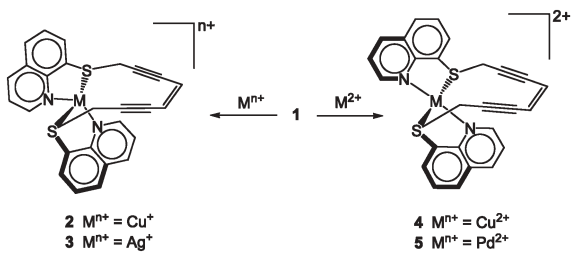

Scheme 2 Synthesis of psuedo-tetrahedral and square planar *trans*-metalloenediyne complexes **2**–**5**.

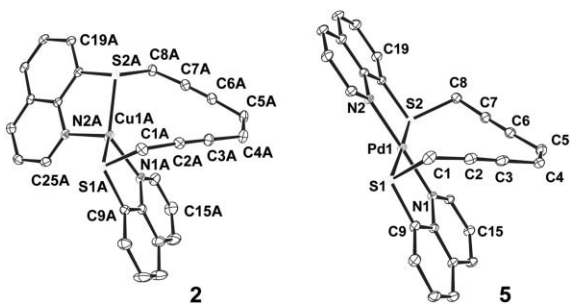

Fig. 1 X-Ray structure of **2** and **5**. Thermal ellipsoids are illustrated at 40% probability. Alkyne termini separation (C2···C7) for **2**: 4.12 Å; **5**: 4.20 Å. M–N bond lengths ~2.04 Å; M–S ~2.3 Å. Counter ions are omitted for clarity.

complex **4** is expected to have a distorted square planar or tetragonal geometry.

The thermal Bergman cyclization reactivities of ligand **1** and the corresponding metalloenediynes **2–5** have been evaluated by a combination of differential scanning calorimetry (DSC) and product isolation studies from cyclization reactions in solution. The thermal reactivity of **1** shows a melting endotherm in the DSC trace at 120 °C that is followed by a large, irreversible exothermic peak at 180 °C characteristic of the cyclization reaction in the neat melt. Free ligand **1** is stable in solution and does not cyclize upon heating at 150 °C in DMSO with 100-fold excess 1,4-cyclohexadiene (CHD) over 8 h. With continued heating, **1** decomposes without formation of cyclized product.

For metalloenediynes **2–5**, heating of solid samples results in large, single exothermic peaks with maxima at ~155 °C for **2** and **3**, and ~130 °C for **4** and **5**, indicating cyclization of the enediyne unit in the solid state. For tetrahedral complexes **2** and **3**, these values are similar to but slightly lower than analogous bidentate chelates,[6] revealing the geometric,[12] and possibly weak electronic[13] assistance of the thioether in cyclization. These complexes are also stable in solution (MeCN/CHD) at 95 °C for 10 h. Continued heating at this temperature causes gradual decomposition of compounds without formation of cyclized product. Heating of the Cu(II) complex **4** in MeCN/CHD for 10 h at 75 °C followed by demetallation with excess EDTA, results in generation of Bergman cyclized product **6** in 15–20% isolated yield along with 30% of free ligand **1**. Heating of **5** in MeCN/CHD at 75 °C for 10 h followed by demetallation with 4 eq pyridine affords 30% of cyclized product **6** without any persistence of unreacted starting materials (Scheme 3). The remaining mass balance (for both cases) consists of insoluble polymeric and decomposed product. Compound **6** was characterized by NMR and mass analysis. Despite repeated attempts, cyclized complex **5** could not be isolated from the reaction mixture in pure form.

The impetus for the design of these complexes was to incorporate a non-rigid binding motif that had the potential to switch molecular conformation en route to formation of the cyclized product. For example, conversion of **4** or **5** from *trans* to *cis*, while the tetrahedral constructs of **2** and **3** serve as geometric structural controls. Simple inspection of **5** and **6** suggests that the *trans* conformation of **5** would not be the most stable form of the cyclized product. The same argument applies to the distorted square planar/tetragonal geometry of the cyclized product of the Cu(II) complex **4**. In addition, the solid-state cyclization temperatures of **4** and **5** are nearly identical and lower than the tetrahedral constructs **2** and **3**. Moreover, the values are in line with the established relationship between tetrahedral and *cis*-planar metalloenediyne geometries,[4–10] and are identical to Cu(II) complexes of similar structure.[3,6,7,9,10,14]

To probe the structure of the cyclized product of **5**, isolated **6** was complexed with $Pd(BF_4)_2$ (1 : 1, RT) and yielded the

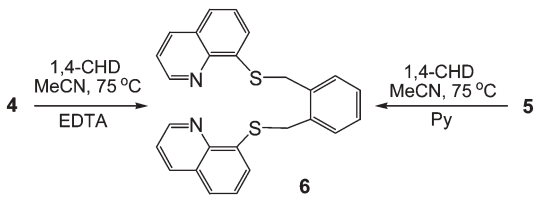

Scheme 3 Bergman cyclization of **4** and **5** in solution.

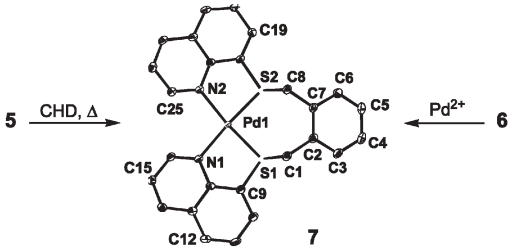

Scheme 4 Bergman cyclization of **5** in solution and X-ray structure of **7**. Thermal ellipsoids are illustrated at 40% probability. Counter ions are omitted for clarity.

cis-planar complex **7**‖ in 90% yield (Scheme 4). The ^{1}H NMR multiplets at δ 6.66 and 6.89 ppm, and ^{13}C resonances at δ 138.67, 131.03, 128.14 ppm correspond to the new aromatic ring and are observed during the cyclization of **5**, supporting the geometric switch from *trans* **5** to *cis* cyclized product.

The thermal reactivities of **4, 5** relative to **2, 3** suggest that the temperature for the cyclization is reduced by a geometrical transformation during the cyclization reaction. This is driven by reduction in the size of the chelate (11-membered to 7-membered), causing the *trans* isomer to be energetically disfavored. To address this issue, density functional theory (DFT) calculations were performed using the Jaguar 6.0 software suite.[15] Geometries and vibrations were calculated using the PWPW91[16,17] functional with the LACV3P** basis set that applies 6-311G** to all light atoms and the Los Alamos effective core potentials[18,19] to palladium. Subsequent single point energy calculations were performed on geometries obtained using this level of theory (see ESI† for Cartesian coordinates) with a correlation consistent, polarized valence triple ζ basis set that excludes f orbitals [cc-pVTZ(-f)].[20] The results confirm the observable; the *trans* starting material (*e.g.* **5**) is ~6–9 kcal mol^{-1} more stable than the *cis* counterpart (Table 1). Part of the energy difference derives from a slight geometric distortion at the Pd(II) center that is required to minimize steric repulsion between the opposing quinoline rings in the *cis* conformation. Importantly, the computations demonstrate that the *cis* geometry is thermodynamically accessible under the reaction conditions, and that a *trans*-to-*cis* interconversion as a prelude to cyclization is energetically reasonable. Since the *cis* isomer is not detected in the course of Bergman product formation, this would suggest that geometry change leads to spontaneous cyclization.

In order to justify this argument, we have synthesized **8**,** which is the benzannulated version of **5**. The thermal stability of **8** is increased relative to **5** due the presence of the aromatic system at the *ene* position. Heating this complex at 80 °C for 10 h in MeCN results in no reaction. Neither cyclization nor the geometrical

Table 1 Structural parameters and computed energies for experimental and calculated structures of **5**

	5 X-ray	**5** calculated	*cis–anti*	*cis–syn*
Pd–S1/Å	2.31	2.36	2.34	2.34
Pd–S2/Å	2.30	2.36	2.34	2.36
Pd–N1/Å	2.04	2.09	2.10	2.14
Pd–N2/Å	2.09	2.09	2.10	2.12
C2–C7/Å	4.22	4.16	3.91	3.91
Energy/kcal mol^{-1}	—	0	6.43	9.36

[a] Geometries calculated using the PWPW91/LACV3P**, energies calculated using PWPW91/cc-pVTZ(-f).

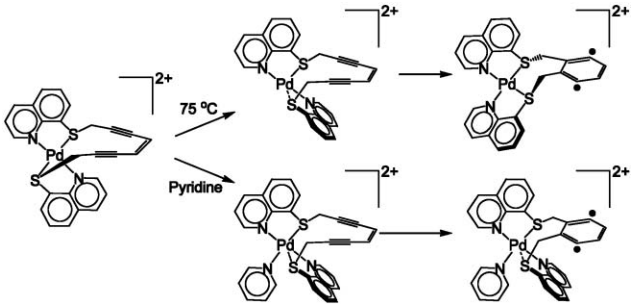

Scheme 5 Proposed thioether dissociation and Pd–N bond rotation mechanism for the *trans*-to-*cis* promoted Bergman cyclization.

change (*trans*-to-*cis*) of the complex are observed by NMR, consistent with the DFT results that the *cis* isomer is not a stable ground state structure, and therefore may be energetically and structurally closer to the transition state of the cyclized product than the *trans* starting material.

Our mechanistic hypothesis is based on the premise that loss of one weakly coordinated thioether ligand provides sufficient driving force to promote a *trans*-to-*cis* (or nearly *cis*) geometry change about the metal, thereby removing the stability of the enediyne associated with the *trans* complex and promoting cyclization. Our observation that 4 eq of pyridine can displace the cyclized ligand and sequester the metal (*cf*. Scheme 4) led to the idea to use 1 eq of pyridine to activate the complex by competitive ligand exchange. Indeed, Minniti has shown that for a normally dissociative *trans*-to-*cis* geometry change which occurs within *trans*-$[Pd(C_6F_5)_2(tht)_2]$ (tht = tetrahydrothiophene) at elevated temperature (60 °C), addition of 1 eq of pyridine can actively promote isomerization under *ambient* conditions by associative substitution.[21]

To this end, addition of 1 eq of pyridine to **5** leads to formation of cyclized product **7** within 2 h at ambient temperature. Displacement of the thioether from Pd^{2+} is identified by an upfield shift in the ^{1}H resonances for the $–CH_2–S–$ linkage from 4.79, 4.46 (second order doublets) to 3.91 ppm. *In situ* cyclized product formation is then identified by the disappearance of the ^{1}H signal from the –CH=CH– unit, customary downfield shift in the resonance for $–CH_2–S–$ fragment (5.10, 4.60 ppm), and additional resonances for the new aromatic ring at 6.66 and 6.89 ppm. Per Scheme 3, cyclized **6** was isolated in 32% yield from the pyridine reaction.

The ability of pyridine to initiate the cyclization reaction *via* thioether dissociation at ambient temperature supports our mechanistic hypothesis that geometric isomerization triggers the cyclization reaction. We propose that upon thioether dissociation, ~90° rotation of the ligand about the adjacent Pd–N bond leads to formation of a weak axial, square pyramidal species (4-coordinate sawhorse geometry in the absence of pyridine), which places the thioethers within a ~90° relationship analogous to that of the *cis* isomer (Scheme 5). The resulting transient then undergoes Bergman cyclization to form the desired product. In the absence of pyridine, elevated temperature is required to promote thioether bond dissociation, allowing rotation about the Pd–N bond and geometric rearrangement to form the *cis* isomer. Subsequent Bergman cyclization then leads to the more stable *cis* product.

The results presented here provide evidence suggesting that non-rigid geometric coordination of an enediyne about a metal within a given oxidation state, can be used as a switch to drive Bergman cyclization by converting stable enediyne conformations to their reactive counterparts. In this capacity, thermal cyclization occurs at ~100 °C below where it would be expected.

The support of the National Institutes of Health (R01 GM62541-01A1) is gratefully acknowledged.

Notes and references

‡ Crystallographic data for **1**: $C_{26}H_{18}N_2S_2$, M = 340.45, triclinic, space group $P\bar{1}$, Z = 2, a = 7.8181(6), b = 11.2558(9), c = 11.7943(9) Å, α = 86.300(2), β = 81.141(2), γ = 88.620(2)°, V = 1023.26(14) Å^3, T = 130(2) K, μ = 0.276 mm^{-1}, unique reflections = 4166 (R_{int} = 0.0341), R_1 (all data) = 0.0422, wR_2 (all data) = 0.0984.

§ Crystallographic data for **2**: $C_{26.75}H_{19.50}N_2Cl_{1.50}CuF_6PS_2$, M = 694.75, triclinic, space group $P\bar{1}$, Z = 4, a = 11.893(3), b = 15.257(4), c = 16.966(4) Å, α = 83.414(6), β = 75.378(6), γ = 68.398(5)°, V = 2768.9(12) Å^3, T = 130(2) K, μ = 1.205 mm^{-1}, unique reflections = 11339 (R_{int} = 0.0432), R_1 (all data) = 0.0697, wR_2 (all data) = 0.1671.

¶ Crystallographic data for **5**: $C_{28}H_{21}B_2F_8N_3PdS_2$, M = 743.62, monoclinic, space group $P2_1/n$, Z = 4, a = 13.2183(14), b = 11.6622(13), c = 18.790(2) Å, β = 93.675(3)°, V = 2890.5(5) Å^3, T = 113(2) K, μ = 0.864 mm^{-1}, unique reflections = 6654 (R_{int} = 0.095), R_1 ($I>2\sigma(I)$) = 0.0314, wR_2 (all data) = 0.0740.

‖ Crystallographic data for **7**: $C_{26}H_{20}B_2F_8N_2PdS_2$, M = 704.58, triclinic, space group $P\bar{1}$, Z = 2, a = 7.9642(5), b = 9.4857(6), c = 17.9043(11) Å, α = 85.756(2), β = 88.366(2), γ = 71.6800(10)°, V = 1280.50(14) Å^3, T = 120(2) K, μ = 1.827 mm^{-1}, unique reflections = 4127 (R_{int} = 0.0304), R_1 ($I>2\sigma(I)$) = 0.0373, wR_2 ($I>2\sigma(I)$) = 0.0952.

CCDC 268256–268259. See http://dx.doi.org/10.1039/b509125j for crystallographic data in CIF or other electronic format.

** Crystallographic data for **8**: $C_{32}H_{23}B_2F_8N_3PdS_2$, M = 793.67, monoclinic, space group $P2_1/c$, Z = 4, a = 14.912(2), b = 11.8170(16), c = 17.597(2) Å, β = 91.245(4)°, V = 3100.0(7) Å^3, T = 120(2) K, μ = 1.701 mm^{-1}, unique reflections = 6299 (R_{int} = 0.0458), R_1 ($I>2\sigma(I)$) = 0.0286, wR_2 ($I>2\sigma(I)$) = 0.0699.

1 A. Basak, S. Mandal and S. S. Bag, *Chem. Rev.*, 2003, **103**, 4077–4094.
2 D. S. Rawat and J. M. Zaleski, *Synlett*, 2004, 393–421.
3 S. Bhattacharyya and J. M. Zaleski, *Curr. Top. Med. Chem.*, 2004, **4**, 1637–1654.
4 B. P. Warner, S. P. Millar, R. D. Broene and S. L. Buchwald, *Science*, 1995, **269**, 814–816.
5 N. L. Coalter, T. E. Concolino, W. E. Streib, C. G. Hughes, A. L. Rheingold and J. M. Zaleski, *J. Am. Chem. Soc.*, 2000, **122**, 3112–3117.
6 P. J. Benites, D. S. Rawat and J. M. Zaleski, *J. Am. Chem. Soc.*, 2000, **122**, 9882.
7 D. S. Rawat, P. J. Benites, C. D. Incarvito, A. L. Rheingold and J. M. Zaleski, *Inorg. Chem.*, 2001, **40**, 1846–1857.
8 E. W. Schmitt, J. C. Huffman and J. M. Zaleski, *Chem. Commun.*, 2001, 167–168.
9 T. Chandra, M. Pink and J. M. Zaleski, *Inorg. Chem.*, 2001, **40**, 5878–5885.
10 T. Chandra, R. A. Allred, B. J. Kraft, L. M. Berreau and J. M. Zaleski, *Inorg. Chem.*, 2004, **43**, 411–420.
11 Y.-Z. Hu, C. Chamchoumis, J. S. Grebowicz and R. P. Thummel, *Inorg. Chem.*, 2002, **41**, 2296–2300.
12 D. S. Rawat and J. M. Zaleski, *J. Am. Chem. Soc.*, 2001, **123**, 9675–9676.
13 S. Bhattacharyya, M. Pink, M.-H. Baik and J. M. Zaleski, *Angew. Chem., Int. Ed.*, 2005, **44**, 592–595.
14 S. Bhattacharyya, E. Clark Aurora, M. Pink and J. M. Zaleski, *Chem. Commun.*, 2003, 1156–1157.
15 *Jaguar, version 6.0*, Schrödinger, LLC, New York, NY, 2005.
16 J. P. Perdew, *Electronic Structure Theory of Solids*, Academie Verlag, Berlin, 1991.
17 J. P. Perdew, J. A. Chevary, S. H. Vosko, K. A. Jackson, M. R. Pederson, D. J. Singh and C. Fiolhais, *Phys. Rev. B*, 1992, **46**, 6671–6687.
18 P. J. Hay and W. R. Wadt, *J. Chem. Phys.*, 1985, **82**, 270–283.
19 P. J. Hay and W. R. Wadt, *J. Chem. Phys.*, 1985, **82**, 299–310.
20 R. A. Kendall, T. H. Dunning, Jr. and R. J. Harrison, *J. Chem. Phys.*, 1992, **96**, 6796–6806.
21 D. Minniti, *Inorg. Chem.*, 1994, **33**, 2631–2634.